Inorg. Chem. **2006**, *45*, 6740–6747

Carbon Dioxide Fixation by an Unprecedented Hydroxo Lead–Chromium Carbonyl Complex: Synthesis, Reactivity, and Theoretical Calculations

Miao-Hsing Hsu,[†] Rung-Tsang Chen,[†] Wen-Shyan Sheu,[‡] and Minghuey Shieh*[,†]

Departments of Chemistry, National Taiwan Normal University, Taipei 116, Taiwan, Republic of China, and Fu-Jen Catholic University, Hsinchuang, Taipei 242, Taiwan, Republic of China

Received April 3, 2006

The novel hydroxo-bridged dimeric lead–chromium carbonyl complex $[Et_4N]_2[\{PbCr_2(CO)_{10}\}_2(\mu\text{-}OH)_2]$ ($[Et_4N]_2$[**1**]) was synthesized from the reaction of $PbCl_2$ and $Cr(CO)_6$ followed by metathesis with $[Et_4N]Br$ in a KOH/MeOH solution. The X-ray crystallographic structure shows that dianion **1** consists of two $Pb\{Cr(CO)_5\}_2$ units bridged by two hydroxo fragments in which the Pb atoms are further coordinated with two $Cr(CO)_5$ groups, resulting in a distorted tetrahedral geometry. A CO_2 molecule can insert itself into dianion **1** to form two new carbonate complexes, $[Et_4N]_2[\{PbCr_2(CO)_{10}\}(CO_3)]$ ($[Et_4N]_2$[**2**]) and $[Et_4N]_2[\{PbCr_2(CO)_{10}\}_2(CO_3)]$ ($[Et_4N]_2$[**3**]), depending on the reaction conditions. In addition, complex **2** can be transformed into **3** in CH_2Cl_2 solution at an elevated temperature. While the carbonate group in dianion **2** is bonded to one Pb atom, which is coordinated with two $Cr(CO)_5$ fragments, the carbonate group in **3** bridges the two Pb centers in a μ-1κ^2OO′:2κ^2OO′ fashion in which each Pb atom is further bonded to two $Cr(CO)_5$ moieties. Complexes **2** and **3** can be converted back the hydroxo complex **1** under appropriate conditions. All three unprecedented lead–chromium compounds, **1**–**3**, were fully characterized by spectroscopic methods and single-crystal X-ray diffraction analyses. The nature and formation of complexes **1**–**3** were also examined by molecular orbital calculations using the B3LYP method of the density functional theory.

Introduction

A great deal of interest has focused on the role of metal ions as active centers in the fixation of CO_2 and its transformation.[1] The fixation of CO_2 by metal complexes is of special interest because a fundamental understanding of such reactions may aid in the developement of some practical means to reduce the levels of CO_2 present in the atmosphere.[2] Further, the activation of CO_2 by hydroxo metal complexes to produce metal bicarbonate or carbonato species is also related to the function of carbonic anhydrase, a metalloenzyme,[3] which catalyzes the physiologically important hydration of CO_2 to bicarbonate. While a wide variety of transition metal compounds are able to form complexes with CO_2, main group organometallic species that are known to bind CO_2 are scarce.[1,2e,4] For main group−transition metal complexes, this issue remains even less explored, mainly, because of the complicated cooperative effects of main group elements and transition metals. One rare example was reported in which the $Sn(OH)_3$-capped trinuclear nickel cluster, $Ni_3(\mu$-

* To whom correspondence should be addressed. E-mail: mshieh@ntnu.edu.tw.

† National Taiwan Normal University.

‡ Fu-Jen Catholic University.

(1) (a) Palmer, D. A.; van Eldik, R. *Chem. Rev.* **1983**, *83*, 651. (b) Leitner, W. *Coord. Chem. Rev.* **1996**, *153*, 257. (c) Darensbourg, D. J.; Holtcamp, M. W. *Coord. Chem. Rev.* **1996**, *153*, 155. (d) Baehr, A. *Carbon Dioxide Activation by Metal Complexes*; VCH: Weinheim, Germany, 1988. (e) Dell'Amico, D. B.; Calderazzo, F.; Labella, L.; Marchetti, F.; Pampaloni, G. *Chem. Rev.* **2003**, *103*, 3857. (f) Yin, X.; Moss, J. R. *Coord. Chem. Rev.* **1999**, *181*, 27. (g) Gibson, D. H. *Chem. Rev.* **1996**, *96*, 2063.

(2) (a) Evans, W. J.; Miller, K. A.; Ziller, J. W. *Inorg. Chem.* **2006**, *45*, 424. (b) Santamaría, D.; Cano, J.; Royo, P.; Mosquera, M. E. G.; Cuenca, T.; Frutos, L. M.; Castaño, O. *Angew. Chem., Int. Ed.* **2005**, *44*, 5828. (c) Kong, L.-Y.; Zhang, Z.-H.; Zhu, H.-F.; Kawaguchi, H.; Okamura, T.-a.; Doi, M.; Chu, Q.; Sun, W.-Y.; Ueyama, N. *Angew. Chem., Int. Ed.* **2005**, *44*, 4352. (d) Xie, H.; Duan, H.; Li, S.; Zhang, S. *New J. Chem.* **2005**, *29*, 1199. (e) Beckmann, J.; Dakternieks, D.; Duthie, A.; Lewcenko, N. A.; Mitchell, C. *Angew. Chem., Int. Ed.* **2004**, *43*, 6683. (f) Natrajan, L.; Pécaut, J.; Mazzanti, M. *Dalton Trans.* **2006**, 1002. (g) García, M. P.; Jiménez, M. V.; Lahoz, F. J.; Oro, L. A. *J. Chem. Soc., Dalton Trans.* **1995**, 917. (h) Kitajima, N.; Hikichi, S.; Tanaka, M.; Moro-oka, Y. *J. Am. Chem. Soc.* **1993**, *115*, 5496.

(3) (a) Peters, J. W. *Science* **2002**, *298*, 552. (b) Cullen, J. T.; Lane, T. W.; Morel, F. M. M.; Sherrell, R. M. *Nature* **1999**, *402*, 165. (c) Schenk, S.; Kesselmeier, J.; Anders, E. *Chem. Eur. J.* **2004**, *10*, 3091. (d) Parkin, G. *Chem. Rev.* **2004**, *104*, 699. (e) Strasdeit, H. *Angew. Chem., Int. Ed.* **2001**, *40*, 707.

(4) (a) Kümmerlen, J.; Sebald, A.; Reuter, H. *J. Organomet. Chem.* **1992**, *427*, 309. (b) Blunden, S. J.; Hill, R.; Ruddick, J. N. R. *J. Organomet. Chem.* **1984**, *267*, C5. (c) Bloodworth, A. J.; Davies, A. G.; Vasishtha, S. C. *J. Chem. Soc. C* **1967**, 1309. (d) Sato, H. *Bull. Chem. Soc. Jpn.* **1967**, *40*, 410.

10.1021/ic060554o CCC: $33.50
Published on Web 07/28/2006

P,P′-$PPh_2CH_2PPh_2)_3(\mu_3$-Cl)(μ_3-Sn$(OH)_3$), was found to react with CO_2 to form the molecular complex $Ni_3(\mu$-P,P′-PPh_2-$CH_2PPh_2)_3(\mu_3$-Cl)(μ_3-Sn(OH)(CO_3)) without interference via the formation of oligomeric tin oxides.[5]

As part of our studies to probe the coupling effects of main group elements and transition metals, we have been interested in developing rational routes to main group-containing transition metal carbonyl complexes, in attempts to study their structural versatility and properties.[6−8] In the chromium-related system, group 15-hydrido trichromium complexes of the type $[HE\{Cr(CO)_5\}_3]^{2-}$ (E = As, Sb)[7] and the dichalcogen-capped trichromium clusters $[E_2Cr_3(CO)_{10}]^{2-}$ (E = Se, Te)[8] have been produced from reactions of main group oxides with $Cr(CO)_6$ under appropriate conditions. These studies demonstrate that the remarkable difference in reactivity between these two classes is closely related to the role of main group elements because of their differing sizes and electronic demands.

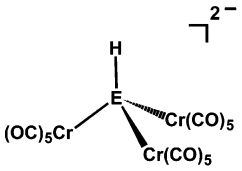

E = As, Sb

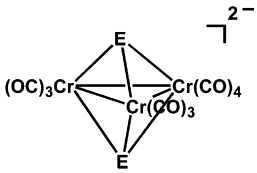

E = Se, Te

The extensive information available on the chemistry of chromium carbonyl species in combination with group 15[7] and group 16[8] elements prompted us to explore group 14-containing chromium carbonyl complexes. In contrast to group 15- and group 16-chromium carbonyl clusters, studies of the class of Pb−Cr−CO complexes have been rare,[9] mainly, because of their reactive nature and the absence of generally applicable synthetic methods. In this paper, we wish to describe a straightforward route to a novel hydroxo-bridged lead−chromium complex $[\{PbCr_2(CO)_{10}\}_2(\mu$-$OH)_2]^{2-}$ (**1**) from the reaction of $PbCl_2$ with $Cr(CO)_6$ in a KOH/MeOH solution. Although a similar type of complexes, $[Ph_4P]_2[\{(CO)_5Cr\}_2Pb(\mu_2$-$OR)_2Pb\{Cr(CO)_5\}_2]$ (R = Et, *n*-Pr, *i*-Pr, allyl),[9b] was reported by Huttner et al. via the substitution of $[\{(CO)_5Cr\}_2Pb(NO_3)_2]^{2-}$ with alkoxides, the hydroxo derivative was not reported, and their chemical reactivity has never been explored. Hydroxo compounds are of particular interest because of their interesting reactivity and potential relevance to catalysis.[2f−h,3,5,10] In this study, we demonstrate the first example of the insertion of CO_2 into the hydroxo lead-containing metal complex. Its reactivity and formation are also investigated and discussed on the basis of DFT calculations.

Experimental Section

All reactions were performed under an atmosphere of pure nitrogen using standard Schlenk techniques.[11] Solvents were purified, dried, and distilled under nitrogen prior to use. $Cr(CO)_6$ (Strem), $PbCl_2$ (Osaka), and KOH (Showa) were used as received. Infrared spectra were recorded on a Perkin-Elmer Paragon 500 IR spectrometer as solutions in CaF_2 cells. The ^1H and ^{13}C NMR spectra were obtained on a JEOL 400 instrument at 399.78 and 100.53 MHz, respectively. Elemental analyses for C, H, and N were performed on a Perkin-Elmer 2400 analyzer at the NSC Regional Instrumental Center at National Taiwan University, Taipei, Taiwan.

Synthesis of $[Et_4N]_2[\{PbCr_2(CO)_{10}\}_2(\mu$-$OH)_2]$ ($[Et_4N]_2$[1]). A mixture of 3.35 g (59.7 mmol) of KOH, 0.38 g (1.37 mmol) of $PbCl_2$, and 0.61 g (2.77 mmol) of $Cr(CO)_6$ was added 20 mL of MeOH in an ice−water bath. The resulting solution was stirred at 35 °C for 3 h to give a reddish brown solution. The solution was filtered and an aqueous solution of 0.50 g (2.38 mmol) of Et_4NBr was added, precipitating the reddish brown product. The product was collected by filtration, washed with deionized water, and dried under vacuum. The CH_2Cl_2 extract was recrystallized from Et_2O/CH_2Cl_2 to give 0.56 g (0.38 mmol) of reddish-brown $[Et_4N]_2[\{PbCr_2(CO)_{10}\}_2(\mu$-$OH)_2]$ ($[Et_4N]_2$[**1**]) (55% based on $PbCl_2$). IR (ν_{CO}, CH_2Cl_2): 3454 br, 2002 m, 1979 s, 1917 s, 1862 m cm^{-1}. Anal. Calcd for $[Et_4N]_2$[**1**]: C, 29.27; H, 2.87; N, 1.90. Found: C, 29.19; H, 2.81; N, 1.87. ^1H NMR (400 MHz, DMSO-d_6, 295 K): δ 7.69 (s, 2H, OH) (chemical shifts not given for $[Et_4N]^+$). Crystals of [TEBA]$_2$[**1**] suitable for X-ray diffraction were grown from Et_2O/CH_2Cl_2.

Synthesis of $[Et_4N]_2[\{PbCr_2(CO)_{10}\}(CO_3)]$ ($[Et_4N]_2$[2]). Carbon dioxide was bubbled through a solution of 0.32 g (0.22 mmol) of $[Et_4N]_2$[**1**] in 30 mL of CH_2Cl_2 in an ice−water bath for 15 min. The color of the solution immediately changed from reddish brown to reddish orange. After the mixture was stirred for another 15 min at 0 °C, the solution was filtered, and the solvent was evaporated under vacuum. The CH_2Cl_2 extract was recrystallized from Et_2O/CH_2Cl_2 to give 0.17 g (0.19 mmol) of reddish orange $[Et_4N]_2[\{PbCr_2(CO)_{10}\}(CO_3)]$ ($[Et_4N]_2$[**2**]) (86% based on $[Et_4N]_2$-[**1**]). IR (ν_{CO}, CH_2Cl_2): 2002 m, 1920 s, 1875 m, 1440 m cm^{-1}. Anal. Calcd for $[Et_4N]_2$[**2**]: C, 35.57; H, 4.42; N, 3.07. Found: C, 35.93; H, 4.19; N, 2.77. ^{13}C NMR (100 MHz, DMSO-d_6, 295 K): δ 165.1 (CO_3), 213.7, 217.2, 221.5, 223.7 (CrCO) (chemical shifts

(5) Simón-Manso, E.; Kubiak, C. P. *Angew. Chem., Int. Ed.* **2005**, *44*, 1125.
(6) (a) Shieh, M.; Chen, P.-F.; Tsai, Y.-C.; Shieh, M.-H.; Peng, S.-M.; Lee, G.-H. *Inorg. Chem.* **1995**, *34*, 2251. (b) Shieh, M.; Shieh, M.-H.; Tsai, Y.-C.; Ueng, C.-H. *Inorg. Chem.* **1995**, *34*, 5088. (c) Huang, K.-C.; Tsai, Y.-C.; Lee, G.-H.; Peng, S.-M.; Shieh, M. *Inorg. Chem.* **1997**, *36*, 4421. (d) Shieh, M.; Chen, H.-S.; Yang, H.-Y.; Ueng, C.-H. *Angew. Chem., Int. Ed. Engl.* **1999**, *38*, 1252. (e) Shieh, M.; Chen, H.-S.; Yang, H.-Y.; Lin, S.-F.; Ueng, C.-H. *Chem.—Eur. J.* **2001**, *7*, 3152. (f) Shieh, M.; Cherng, J.-J.; Lai, Y.-W.; Ueng, C.-H.; Peng, S.-M.; Liu, Y.-H. *Chem.—Eur. J.* **2002**, *8*, 4522. (g) Shieh, M.; Chung, R.-L.; Yu, C.-H.; Hsu, M.-H.; Ho, C.-H.; Peng, S.-M.; Liu, Y.-H. *Inorg. Chem.* **2003**, *42*, 5477.
(7) (a) Cherng, J.-J.; Lee, G.-H.; Peng, S.-M.; Ueng, C.-H.; Shieh, M. *Organometallics* **2000**, *19*, 213. (b) Cherng, J.-J.; Lai, Y.-W.; Liu, Y.-H.; Peng, S.-M.; Ueng, C.-H.; Shieh, M. *Inorg. Chem.* **2001**, *40*, 1206.
(8) (a) Shieh, M.; Ho, L.-F.; Jang, L.-F.; Ueng, C.-H.; Peng, S.-M.; Liu, Y.-H. *Chem. Commun.* **2001**, 1014. (b) Shieh, M.; Lin, S.-F.; Guo, Y.-W.; Hsu, M.-H.; Lai, Y.-W. *Organometallics* **2004**, *23*, 5182. (c) Hsu, M.-H.; Miu, C.-Y.; Lin, Y.-C.; Shieh, M. *J. Organomet. Chem.* **2006**, *691*, 966.
(9) (a) Rutsch, P.; Huttner, G. *Angew. Chem., Int. Ed.* **2000**, *39*, 2118. (b) Rutsch, P.; Huttner, G. *Z. Naturforsch. B.* **2002**, *57*, 25. (c) Kircher, P.; Huttner, G.; Heinze, K.; Schiemenz, B.; Zsolnai, L.; Büchner, M.; Driess, A. *Eur. J. Inorg. Chem.* **1998**, 703. (d) Kircher, P.; Huttner, G.; Schiemenz, B.; Heinze, K.; Zsolnai, L.; Walter, O.; Jacobi, A.; Driess, A. *Chem. Ber.* **1997**, *130*, 687. (e) Seidel, N.; Jacob, K.; Fischer, A. K. *Organometallics* **2001**, *20*, 578. (f) Pu, L.; Power, P. P.; Boltes, I.; Herbst-Irmer, R. *Organometallics* **2000**, *19*, 352. (g) Eichhorn, B. W.; Haushalter, R. C. *Chem. Commun.* **1990**, 937.
(10) (a) Sakamoto, K.; Hamada, Y.; Akashi, H.; Orita, A.; Otera, J. *Organometallics* **1999**, *18*, 3555. (b) Cervini, R.; Fallon, G. D.; Spiccia, L. *Inorg. Chem.* **1991**, *30*, 831.
(11) Shriver, D. F.; Drezdon, M. A. *The Manipulation of Air-Sensitive Compounds*; Wiley-VCH Publishers: New York, 1986.

Table 1. Crystallographic Data for $[TEBA]_2[\{PbCr_2(CO)_{10}\}_2(\mu\text{-}OH)_2]$ ($[TEBA]_2$[**1**]), $[TMBA]_2[\{PbCr_2(CO)_{10}\}(CO_3)]$ ($[TMBA]_2$[**2**]), and $[Et_4N]_2[\{PbCr_2(CO)_{10}\}_2(CO_3)]$ ($[Et_4N]_2$[**3**])

	$[TEBA]_2$[**1**]	$[TMBA]_2$[**2**]	$[Et_4N]_2$[**3**]
empirical formula	$C_{46}H_{46}Cr_4N_2O_{22}Pb_2$	$C_{31}H_{32}Cr_2N_2O_{13}Pb$	$C_{37}H_{40}Cr_4N_2O_{23}Pb_2$
fw	1601.26	951.79	1503.11
cryst syst	triclinic	monoclinic	monoclinic
space group	$P\bar{1}$	$P2_1/c$	$C2/c$
cryst dimensions (mm)	0.36 × 0.30 × 0.27	0.40 × 0.15 × 0.10	0.14 × 0.10 × 0.05
a (Å)	10.283(6)	12.088(8)	22.5661(5)
b (Å)	12.198(3)	23.971(1)	10.4650(2)
c (Å)	12.236(4)	12.832(5)	22.5559(6)
α (deg)	83.05(3)		
β (deg)	78.77(3)	90.49(4)	90.3523(9)
γ (deg)	69.06(4)		
V (Å^3)	1404(1)	3718(3)	5326.6(2)
Z	1	4	4
D_{calcd} (g cm^{-3})	1.894	1.700	1.874
μ (mm^{-1})	6.798	5.153	7.161
diffractometer	Nonius (CAD4)	Nonius (CAD4)	Nonius (Kappa CCD)
radiation (λ) (Å)	0.71073	0.71073	0.71073
temp (K)	298	298	298
θ range for data collection (deg)	1.70−24.92	1.68−25.92	2.15−24.99
T_{min}/T_{max}	0.09/0.16	0.40/0.59	0.47/0.53
no. of independent reflns	4933 ($I > 2\sigma(I)$)	7282 ($I > 2\sigma(I)$)	4660 ($I > 2\sigma(I)$)
R1[a]/wR2[a]	0.033/0.088 ($I > 2\sigma(I)$)	0.047/0.108 ($I > 2\sigma(I)$)	0.040/0.097 ($I > 2\sigma(I)$)
R1[a]/wR2[a] (all data)	0.041/0.091 ($I > 2\sigma(I)$)	0.162/0.142 ($I > 2\sigma(I)$)	0.071/0.132 ($I > 2\sigma(I)$)

[a] The functions minimized during least-squares cycles were $R1 = \sum||F_o| - |F_c||/\sum F_o$ and $wR2 = [\sum[w(F_o^2 - F_c^2)^2]/\sum[w(F_o^2)^2]]^{1/2}$.

not given for $[Et_4N]^+$). Crystals of $[TMBA]_2$[**2**] suitable for X-ray diffraction were grown from Et_2O/CH_3CN.

Synthesis of $[Et_4N]_2[\{PbCr_2(CO)_{10}\}_2(CO_3)]$ ($[Et_4N]_2$[3]). A solution of 0.31 g (0.21 mmol) of $[Et_4N]_2$[**1**] in 15 mL of CH_2Cl_2 was warmed to 35 °C, bubbled with carbon dioxide for 15 min, and stirred for 6 h to give an orange solution, which was filtered, and the solvent was evaporated under vacuum. The residue of the CH_2Cl_2 extract was recrystallized with Et_2O/CH_2Cl_2 to give 0.09 g (0.06 mmol) of orange $[Et_4N]_2[\{PbCr_2(CO)_{10}\}_2(CO_3)]$ ($[Et_4N]_2$[**3**]) (29% based on $[Et_4N]_2$[**1**]). IR (ν_{CO}, CH_2Cl_2): 2018 s, 1967 m, 1923 vs, 1437 m cm^{-1}. Anal. Calcd for $[Et_4N]$[**3**]: C, 29.52; H, 2.68; N, 1.86. Found: C, 29.31; H, 2.75; N, 1.78. ^{13}C NMR (100 MHz, DMSO-d_6, 295 K): δ 166.8 (CO_3), 220.8, 224.3, 230.7 (CrCO) (chemical shifts not given for $[Et_4N]^+$). Crystals suitable for X-ray diffraction were grown from Et_2O/CH_2Cl_2. The reaction solution was also filtered and precipitated with $BaCl_2$ to give 0.011 g (0.056 mmol) of $BaCO_3$ (27% based on $[Et_4N]_2$[**1**]), which was identified by IR spectra.

Conversion of $[Et_4N]_2$[2] to $[Et_4N]_2$[3]. Fifteen milliliters of CH_2Cl_2 was added to a sample of 0.30 g (0.33 mmol) of $[Et_4N]_2$[**2**]. The reddish orange solution was stirred at 35 °C for 6 h to give an orange solution, which was filtered, and the solvent was evaporated under vacuum. The CH_2Cl_2 extract was recrystallized from Et_2O/CH_2Cl_2 to give 0.17 g (0.11 mmol) of orange $[Et_4N]_2[\{PbCr_2(CO)_{10}\}_2(CO_3)]$ ($[Et_4N]_2$[**3**]) (67% based on $[Et_4N]_2$[**2**]). The released carbonate in the reaction solution was precipitated by Ba^{2+} to form 0.02 g (0.10 mmol) of $BaCO_3$ (61% based on $[Et_4N]_2$[**2**]), which was identified by IR spectra.

Reaction of $[Et_4N]_2$[2] with KOH in MeOH. Eighteen milliliters of MeOH was added to a sample of 0.43 g (0.47 mmol) of $[Et_4N]_2$[**2**]. The solution was treated with 2.5 mL of 0.2 M KOH/MeOH in an ice−water bath, and the mixture was warmed to 35 °C and stirred for 1.5 h to give a reddish brown solution. The solution was filtered, and the solvent was evaporated under vacuum. The CH_2Cl_2 extract was recrystallized from Et_2O/CH_2Cl_2 to give 0.15 g (0.10 mmol) of $[Et_4N]_2[\{PbCr_2(CO)_{10}\}_2(\mu\text{-}OH)_2]$ ($[Et_4N]_2$[**1**]) (43% based on $[Et_4N]_2$[**2**]). The released carbonate in the reaction solution was precipitated by Ba^{2+} to form 0.041 g (0.21 mmol) of $BaCO_3$ (45% based on $[Et_4N]_2$[**2**]), which was identified by IR spectra.

Reaction of $[Et_4N]_2$[3] with KOH in MeOH. Seventeen milliliters of MeOH was added to a sample of 0.43 g (0.29 mmol) of $[Et_4N]_2$[**3**]. The solution was treated with 3 mL of 0.2 M KOH/MeOH in an ice−water bath and stirred for 40 min to give a reddish brown solution. The solution was filtered, and the solvent was removed under vacuum. The CH_2Cl_2 extract was recrystallized from Et_2O/CH_2Cl_2 to give 0.27 g (0.18 mmol) of $[Et_4N]_2[\{PbCr_2(CO)_{10}\}_2(\mu\text{-}OH)_2]$ ($[Et_4N]_2$[**1**]) (62% based on $[Et_4N]_2$[**3**]). The released carbonate in the reaction solution was precipitated by Ba^{2+} to form 0.037 g (0.19 mmol) of $BaCO_3$ (66% based on $[Et_4N]_2$[**3**]), which was identified by IR spectra.

X-ray Structural Characterization of $[TEBA]_2$[1], $[TMBA]_2$[2], and $[Et_4N]_2$[3]. Some selected crystallographic data for $[TEBA]_2$[**1**], $[TMBA]_2$[**2**], and $[Et_4N]_2$[**3**] are given in Table 1. All crystals were mounted on glass fibers with epoxy cement. Data collection for $[TEBA]_2$[**1**] and $[TMBA]_2$[**2**] was carried out using a Nonius (CAD-4) diffractometer with graphite-monochromated Mo Kα radiation at 298 K in the 2θ range of 2.0−50° employing $\theta-2\theta$ scans, and an empirical absorption correction by azimuthal (ψ) scans was applied.[12] Data collection for $[Et_4N]_2$[**3**] was carried out using a Brucker-Nonius Kappa CCD diffractometer with graphite-monochromated Mo Kα radiation at 298 K employing the $\theta-2\theta$ scan mode, and an empirical absorption correction by multiscans was applied. The structures of $[TEBA]_2$[**1**], $[TMBA]_2$[**2**], and $[Et_4N]_2$[**3**] were refined with the SHELXL packages.[13] All of the non-hydrogen atoms for $[TEBA]_2$[**1**], $[TMBA]_2$[**2**], and $[Et_4N]_2$[**3**] were refined with anisotropic temperature factors. The hydrogen atom on the hydroxo group of $[TEBA]_2$[**1**] was calculated and isotropically fixed in the final refinement cycle. Additional crystallographic data in the form of CIF files are available as Supporting Information.

(12) North, A. C. T.; Philips, D. C.; Mathews, F. S. *Acta Crystallogr.* **1968**, *A24*, 351.
(13) Sheldrick, G. M. *SHELXL97*, version 97-2; University of Göttingen: Göttingen, Germany, 1997.

Scheme 1

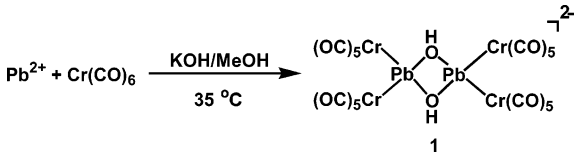

Computational Details. The calculations reported in this study were performed via density functional theory[14] using the Gaussian 03 series of packages.[15] The geometries of complexes **1**−**3** were taken from the crystal structures without further modification. To understand the reactions among complexes **1**−**3**, the geometries of OH^- and CO_3^{2-} were also found by optimization. The optimized geometries of OH^- and CO_3^{2-} were confirmed by the harmonic vibrational frequency analysis, obtained via analytical-energy second derivatives. Natural charges[16] were evaluated using the Weinhold NBO method.[17] All calculations were performed using the LanL2DZ basis sets, the Becke-3-parameter density functional theory (DFT), and the Lee−Yang−Parr correlation functional (B3LYP). Graphical representations of the molecular orbitals were obtained using Gaussview 3.0.

Results and Discussion

Syntheses and Characterizations. Although the use of main group oxides with $Cr(CO)_6$ in MeOH worked well in group 15- and group 16-containing chromium carbonyl complexes, similar strategies were not feasible for lead−chromium carbonyl complexes. By varying the sources of the lead ions and bases and the concentration of the base, we discovered that $PbCl_2$ could readily react with chromium hexacarbonyl in concentrated KOH methanolic solutions at 35 °C followed by metathesis with $[Et_4N]Br$ to give the dihydroxo−lead−chromium complex $[Et_4N]_2[\{PbCr_2(CO)_{10}\}_2(\mu\text{-}OH)_2]$ ($[Et_4N]_2[\mathbf{1}]$) (Scheme 1). This reaction proceeded smoothly, producing $[Et_4N]_2[\mathbf{1}]$ as deep brown air-sensitive crystals in a moderate yield. Like the reactions of $Cr(CO)_6$ with main group oxides in basic solutions,[6f−g,7−8] the reactive species for this reaction were proposed to be $[HCr(CO)_5]^-$/$[Cr(CO)_5]^{2-}$,[18] which could react with Pb^{2+} ions in KOH/MeOH to give complex **1**. An X-ray analysis shows that dianion **1** possesses two $Pb\{Cr(CO)_5\}_2$ units bridged by two hydroxo groups. The existence of hydroxo groups was confirmed by the IR absorption of the hydroxy group at 3454 cm^{-1} and by the ^1H NMR signal at δ 7.69 (2H, OH). These values are in agreement with previously reported values for hydroxo complexes.[19]

Scheme 2

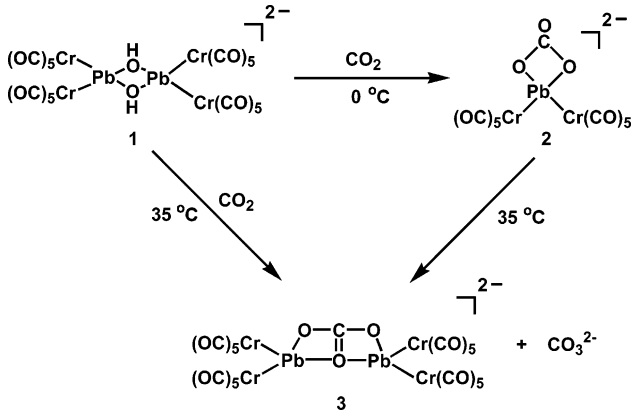

The μ-OH group of compound **1** exhibits nucleophilic addition to carbon dioxide (Scheme 2). Bubbling CO_2 through a solution of complex **1** in CH_2Cl_2 at 0 °C resulted in the formation of the κ^2OO-carbonate complex $[Et_4N]_2[\{PbCr_2(CO)_{10}\}(CO_3)]$ ($[Et_4N]_2[\mathbf{2}]$) in an 86% yield. On the other hand, when the reaction solution was heated at 35 °C and bubbled with CO_2, surprisingly, the new μ-1κ^2OO′:2κ^2OO′-carbonate complex $[Et_4N]_2[\{PbCr_2(CO)_{10}\}_2(CO_3)]$ ($[Et_4N]_2[\mathbf{3}]$) was produced. The results indicate that both carbonato complexes **2** and **3** are CO_2 insertion products from the hydroxo complex **1** under different reaction conditions. In addition, a mixture of complexes **2** and **3** was produced if the CO_2 insertion reaction was conducted at room temperature. We wondered if complexes **2** and **3** could be obtained directly from the reaction of **1** with carbonate. It turned out that the reaction of complex **1** with K_2CO_3 in CH_2Cl_2 did not result in the formation of compound **2** or **3**.

On the basis of its structural features, complex **2** adopts a distorted tetrahedral geometry about the central Pb atom which is bonded to a κ^2OO−CO_3 group and two $Cr(CO)_5$ fragments. In complex **3**, two $Pb\{Cr(CO)_5\}_2$ units are linked with a CO_3 ligand in a μ-1κ^2OO′:2κ^2OO′ bonding mode. The existence of the carbonate ligands in **2** and **3** was further investigated by IR and NMR spectroscopy. Strong carbonate-related vibrations were observed at 1440 cm^{-1} for **2** and at 1437 cm^{-1} for **3**.[2c,20] The presence of a carbonate moiety was also evident from the ^{13}C NMR spectra which showed a signal at 165.1 ppm for **2** and a signal at 166.8 ppm for **3**.

To better understand the reaction pathways, the CO_2 insertion reactions were carefully monitored (Scheme 2). It was found that the reaction of complex **1** in CH_2Cl_2 at 0 °C produced **2** as the only product with no observation of **3**, while the reaction at 35 °C formed both **2** and **3** immediately, which was detected by IR spectroscopy, and then **2** was

(14) Frisch, M. J.; Trucks, G. W.; Schlegel, H. B.; Scuseria, G. E.; Robb, M. A.; Cheeseman, J. R.; Montgomery, J. A., Jr.; Vreven, T.; Kudin, K. N.; Burant, J. C.; Millam, J. M.; Iyengar, S. S.; Tomasi, J.; Barone, V.; Mennucci, B.; Cossi, M.; Scalmani, G.; Rega, N.; Petersson, G. A.; Nakatsuji, H.; Hada, M.; Ehara, M.; Toyota, K.; Fukuda, R.; Hasegawa, J.; Ishida, M.; Nakajima, T.; Honda, Y.; Kitao, O.; Nakai, H.; Klene, M.; Li, X.; Knox, J. E.; Hratchian, H. P.; Cross, J. B.; Bakken, V.; Adamo, C.; Jaramillo, J.; Gomperts, R.; Stratmann, R. E.; Yazyev, O.; Austin, A. J.; Cammi, R.; Pomelli, C.; Ochterski, J. W.; Ayala, P. Y.; Morokuma, K.; Voth, G. A.; Salvador, P.; Dannenberg, J. J.; Zakrzewski, V. G.; Dapprich, S.; Daniels, A. D.; Strain, M. C.; Farkas, O.; Malick, D. K.; Rabuck, A. D.; Raghavachari, K.; Foresman, J. B.; Ortiz, J. V.; Cui, Q.; Baboul, A. G.; Clifford, S.; Cioslowski, J.; Stefanov, B. B.; Liu, G.; Liashenko, A.; Piskorz, P.; Komaromi, I.; Martin, R. L.; Fox, D. J.; Keith, T.; Al-Laham, M. A.; Peng, C. Y.; Nanayakkara, A.; Challacombe, M.; Gill, P. M. W.; Johnson, B.; Chen, W.; Wong, M. W.; Gonzalez, C.; Pople, J. A. *Gaussian 03*, revision B.04; Gaussian, Inc.: Wallingford, CT, 2004.
(15) (a) Becke, A. D. *J. Chem. Phys.* **1993**, *98*, 5648. (b) Lee, C.; Yang, W.; Parr, R. G. *Phys. Rev. B* **1988**, *37*, 785.
(16) (a) Reed, A. E.; Weinhold, F. *J. Chem. Phys.* **1983**, *78*, 4066. (b) Reed, A. E.; Weinstock, R. B.; Weinhold, F. *J. Chem. Phys.* **1985**, *83*, 735.
(17) Reed, A. E.; Curtiss, L. A.; Weinhold, F. *Chem. Rev.* **1988**, *88*, 899.
(18) Darensbourg, M. Y.; Deaton, J. C. *Inorg. Chem.* **1981**, *20*, 1644.
(19) (a) Chandrasekhar, V.; Gopal, K.; Nagendran, S.; Singh, P.; Steiner, A.; Zacchini, S.; Bickley, F. J. *Chem.—Eur. J.* **2005**, *11*, 5437. (b) Twamley, B.; Power, P. P. *Chem. Commun.* **1999**, 1805.
(20) Schrodt, A.; Neubrand, A.; van Eldik, R. *Inorg. Chem.* **1997**, *36*, 4579.

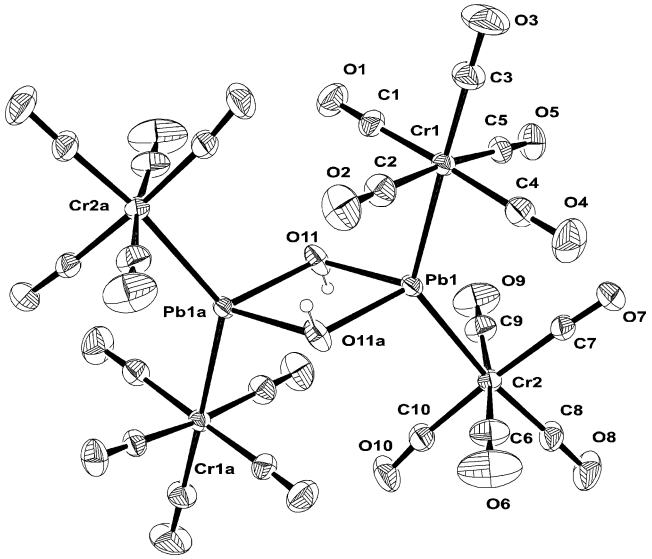

Figure 1. ORTEP diagram of anion **1**, showing 30% probability thermal ellipsoids. Selected bond lengths (Å) and angles (deg): Pb(1)−Cr(1) = 2.680(1), Pb(1)−Cr(2) = 2.708(2), Pb(1)−O(11) = 2.342(4), Pb(1)−O(11a) = 2.320(4), Cr(1)−Pb(1)−Cr(2) = 132.25(4), Cr(1)−Pb(1)−O(11) = 104.9(1), Cr(2)−Pb(1)−O(11) = 111.72(1), Pb(1)−O(11)−Pb(1a) = 103.8(2), O(11)−Pb(1)−O(11a) = 76.3(2).

Scheme 3

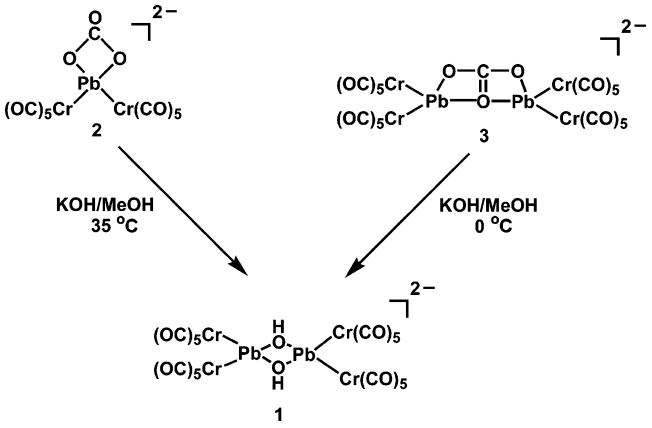

completely transformed to **3** with the formation of the carbonate in the similar yield. The presence of the carbonate was confirmed by the addition of Ba^{2+} to form $BaCO_3$, which was verified by its solid-state IR spectrum. Supported by DFT calculations (discussed later), it is likely that the formation of complex **2** results from the nucleophilic attack of the hydroxo group of complex **1** on the electrophilic carbon of CO_2, accompanied by the Pb−O bond formation, followed by the elimination of the rest of the complex. On the other hand, complex **3** can be considered to be derived from the intermolecular nucleophilic attack of the oxygen atom of CO_3^{2-} of **2** onto the other Pb center of **2** followed by the loss of one carbonate group, as is shown by the initial observation of **2** by IR spectroscopy and the relatively lower yields of **3** and carbonate in the reaction of **1** with CO_2 at 35 °C. Accordingly, we wondered if complex **2** could be converted to complex **3** under controlled conditions. It was indeed the case. Complex **2** was readily transformed to complex **3** in a CH_2Cl_2 solution at 35 °C in an ~70% yield with the formation of the carbonate in a similar yield.

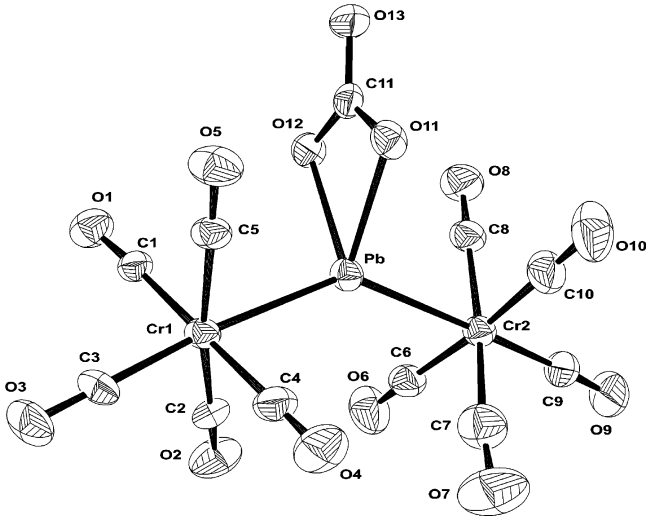

Figure 2. ORTEP diagram of anion **2**, showing 30% probability thermal ellipsoids. Selected bond lengths (Å) and angles (deg): Pb(1)−Cr(1) = 2.657(2), Pb(1)−Cr(2) = 2.671(2), Pb(1)−O(11) = 2.293(7), Pb(1)−O(12) = 2.321(7), C(11)−O(11) = 1.29(1), C(11)−O(12) = 1.31(1), C(11)−O(13) = 1.25(1), Cr(1)−Pb(1)−Cr(2) = 140.49(5), Cr(1)−Pb(1)−O(11) = 111.1(2), Cr(1)−Pb(1)−O(12) = 105.9(2), Cr(2)−Pb(1)−O(11) 104.4(2), Cr(2)−Pb(1)−O(12) = 107.8(2), O(11)−Pb(1)−O(12) = 56.9(2), Pb(1)−O(11)−C(11) = 94.8(6), Pb(1)−O(12)−C(11) = 93.0(6), O(11)−C(11)−O(12) = 115.2(9), O(11)−C(11)−O(13) = 123(1), O(12)−C(11)−O(13) = 122(1).

Moreover, the recovery of the reactive species for the absorption of CO_2 under mild conditions is important for their potential uses. None of the carbonato complexes **2** and **3** were converted into the hydroxo complex **1** when they were simply stirred in CH_2Cl_2 solution in the presence of H_2O. However, we found that the conversion of carbonato complexes **2** and **3** to the hydroxo complex **1** could be achieved under appropriate conditions. When carbonato complex **2** or **3** was treated with diluted KOH in a methanol solution at 35 °C or at 0 °C, both carbonato complexes could be converted back into the hydroxo complex **1** (Scheme 3) in 43 and 62% yields, respectively. Further, the released carbonate for both reactions was determined gravimetrically as $BaCO_3$ (yields of 45 and 66%). By considering the isolated products in these two reactions, we can write their balanced equations as eqs 1 and 2. However, on the basis of the moderate yields for these two reactions, other more complicated reaction pathways and decomposition processes cannot be excluded.

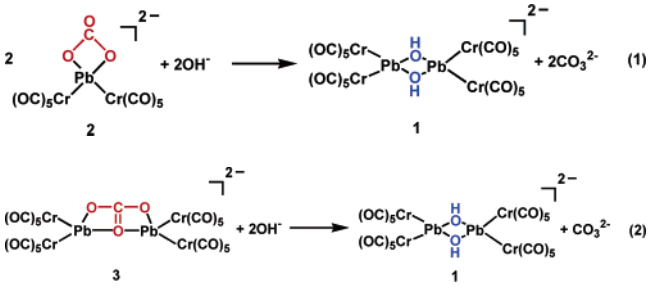

Crystal Structures. The structures of **1**−**3** are shown in Figures 1−3, respectively. As shown in Figure 1, complex **1** contains an inversion center at the center of the Pb_2O_2 planar ring, in which the O(11)−Pb−O(11a) and Pb(1)−

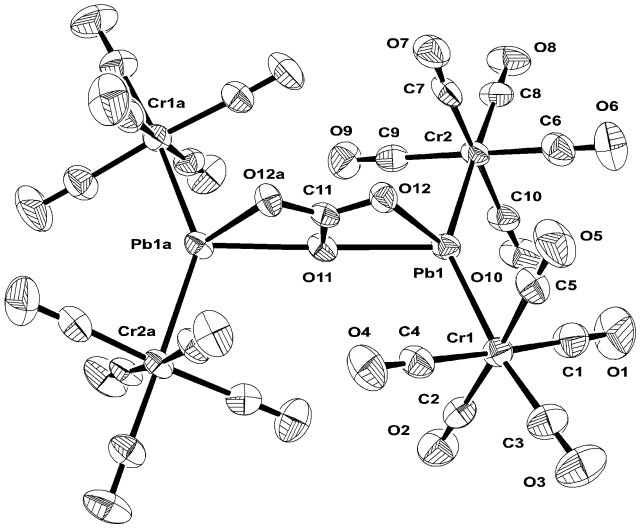

Figure 3. ORTEP diagram of anion **3**, showing 30% probability thermal ellipsoids. Selected bond lengths (Å) and angles (deg): Pb(1)−Cr(1) = 2.643(2), Pb(1)−Cr(2) = 2.645(2), Pb(1)−O(11) = 2.5024(4), Pb(1)−O(12) = 2.321(5), C(11)−O(11) = 1.31(1), C(11)−O(12) = 1.281(7), Cr(1)−Pb(1)−Cr(2) = 142.70(4), Cr(1)−Pb(1)−O(11) = 110.18(3), Cr(1)−Pb(1)−O(12) = 100.0(1), Cr(2)−Pb(1)−O(11) = 106.56(4), Cr(2)−Pb(1)−O(12) = 106.1(1), O(11)−Pb(1)−O(12) = 54.9(2), Pb(1)−O(11)−Pb(1a) = 176.9(3), Pb(1)−O(11)−C(11) = 88.5(2), Pb(1)−O(12)−C(11) = 97.3(5), O(11)−C(11)−O(12) = 119.2(5), O(12)−C(11)−O(12a) = 122(1).

O(11)−Pb(1a) angles are 76.3(2) and 103.8(2)°, respectively. The data also show that the four coordinating $Cr(CO)_5$ groups are in a plane nearly perpendicular to the Pb_2O_2 ring, with the dihedral angle of Pb_2O_2 and Cr_4 being 89.6°. Compound **1** may be considered as being composed of two $[\{(CO)_5Cr\}_2Pb(OH)]^-$ species which are dimerized by oxygen-donor−lead-acceptor bonding to form a four-membered Pb_2O_2 ring because of the electron deficiency at the Pb centers. A similar four-membered Pb_2O_2 heterocycle was observed in the case of $[Ph_4P]_2[\{(CO)_5Cr\}_2Pb(\mu_2\text{-}OR)_2Pb\{Cr(CO)_5\}_2]$ (R = Et, *n*-Pr, *i*-Pr, allyl).[9b] The Pb−O bond lengths (2.320(4) and 2.342(4) Å) in **1** are comparable to those reported for $[Ph_4P]_2[\{(CO)_5Cr\}_2Pb(\mu_2\text{-}OR)_2Pb\{Cr(CO)_5\}_2]$ (R = Et, *n*-Pr, *i*-Pr, allyl) (2.284(3)−2.323(3) Å).[9b] The Pb−Cr distances (2.680(1) and 2.708(2) Å) in **1** are also close to those reported for $[Ph_4P]_2[\{(CO)_5Cr\}_2Pb(\mu_2\text{-}OR)_2Pb\{Cr(CO)_5\}_2]$ (R = Et, *n*-Pr, *i*-Pr, allyl) (average = 2.7042, 2.7079, 2.7332, and 2.7009 Å).[9b] However, the Cr−Pb−Cr angle observed for **1** (132.25(4)°) is larger than those in $[Ph_4P]_2[\{(CO)_5Cr\}_2Pb(\mu_2\text{-}OR)_2Pb\{Cr(CO)_5\}_2]$ (R = Et, *n*-Pr, *i*-Pr, allyl) (125.96(6), 131.20(2), 126.85(3), and 126.67(3)°)[9b] because of the decreased level of steric hindrance of the hydrogen versus the organic groups.

As can be seen in Figure 2, complex **2** contains a central Pb atom bonded to two $Cr(CO)_5$ groups and one carbonate moiety. The carbonate group is apparently distorted from the ideal D_{3h} symmetry (ideal, all C−O ≈ 1.28−1.29 Å)[5] with longer C−O bond lengths for the oxygen atoms coordinated to lead (average = 1.30 Å) and short C−O bond lengths for the uncoordinated oxygen atom (1.25(1) Å). The O(11)−C(11)−O(12) bond angle is narrow (115.2(9)°), reflecting a strained four-membered PbOCO ring with a mean deviation of 0.002 Å from the ideal plane. Some of the interesting features of this PbOCO ring include the rather short nonbonded O−O and Pb−C distances. The O(11)−O(12) separation (2.20 Å) is markedly shorter than the sum of the van der Waals radii (3.00 Å), and the Pb−C(11) separation (2.73 Å) is also evidently shorter than the sum of the van der Waals radii (3.65 Å).[21]

As shown in Figure 3, it is noteworthy that the carbonate moiety in **3** is coordinated to the Pb centers in a $\mu\text{-}1\kappa^2OO'\text{:}2\kappa^2OO'$ manner. The carbonate fragment itself is also distorted from the D_{3h} symmetry, the origin of which appears to be the chelating mode of the carbonate. In contrast to that found for the uncoordinated O atom of the carbonate in complex **2**, further coordination of O(11) to two lead centers is reflected in an increased C(11)−O(11) distance (1.31(1) Å) relative to the C(11)−O(12) and C(11)−O(12a) distances (1.281(7) Å). The $\mu\text{-}1\kappa^2OO'\text{:}2\kappa^2OO'$ bonding mode of this carbonate fragment has been reported for some other transition metal compounds such as $LCuCl(CO_3)ClCuL$ (L = *N*,*N*,*N*′,*N*′-tetramethyl-1,3-propanediamine),[22] $[Cu(L)]_2\text{-}CO_3^{2+}$ (L = 2,4,4,9-tetramethyl-1,5,9-triazacyclododec-1-ene),[23] $[\{Rh(C_6F_5)_3\}_2(\mu\text{-}CO_3)]^{2-}$,[2g] and $LM(\mu\text{-}CO_3)ML$ (M = Mn, Fe, Co, Ni, Cu; L = $HB(3,5\text{-}i Pr_2pz)_3$).[2h] Interestingly, the two lead atoms and the carbonato ligand form a six-membered plane, in which the atoms have a mean deviation of 0.012 Å. The four $Cr(CO)_5$ groups also sit in a plane vertical to the PbOC(O)OPb ring, with the dihedral angle of the two planes being 90.0°.

The Cr−Pb−Cr angles in **2** and **3** are 140.49(5) and 142.70(4)°, respectively, significantly larger than the corresponding angles in $[PPh_4]_2[\{(CO)_5Cr\}_3Pb]$ (average = 119.5°),[9a] $\{(CO)_5Cr\}_2Pb(PR_3)_2$ (R = Me, Et, *n*-Bu) (129.24(3), 129.80(3), and 127.73(5)°),[9b] and complex **1** (132.25(4)°) but shorter than those in $[\{(CO)_5Cr\}_2Pb(OOCMe)_2]^{2-}$ (147.85(5)°)[9d] and $[PPh_4]_2[\{(CO)_5Cr\}_2Pb(NO_3)_2]$ (153.6(4)°),[9b] reflecting the steric effect of the substituents of the Pb atom on the Cr−Pb−Cr angle. It is noteworthy that the sum of the single-bonded metallic radii for lead (1.54 Å)[24] and the metallic radius of chromium (1.29 Å)[24] predicts the bond length of 2.83 Å for the Pb−Cr bond. Thus, the average Pb−Cr distances in **2** and **3** (2.664 and 2.644 Å) are short but comparable to that in **1** (2.694 Å). These lengths are even shorter than the Pb−Cr bonds (average = 2.729 Å) in the planar complex $[Pb\{Cr(CO)_5\}_3]^{2-}$,[9a] indicative of the multiple-bonding character of the Pb−Cr bonds in **1**−**3**.[9e]

In summary, complexes **1**−**3** are rare examples of lead−chromium carbonyl complexes. A search of the Cambridge Crystallographic Data Centre failed to yield any structurally characterized compound with a $Pb_2(\mu\text{-}OH)_2$, a $Pb(\kappa^2OO\text{-}CO_3)$, or a $Pb_2(\mu\text{-}CO_3)$ fragment. Complexes **1**−**3** represent the first examples of such groups. In particular, the presence of the $Pb_2(\mu\text{-}OH)_2$ fragment in complex **1** illustrates the surprising activity for the CO_2 absorption.

(21) (a) Bondi, A. *J. Phys. Chem.* **1964**, *68*, 441. (b) Allinger, N. L.; Hirsch, J. A.; Miller, M. A.; Tyminski, I. J.; Van-Catledge, F. A. *J. Am. Chem. Soc.* **1968**, *90*, 1199.
(22) Churchill, M. R.; Davies, G.; El-Sayed, M. A.; El-Shazly, M. F.; Hutchinson, J. P.; Rupich, M. W.; Watkins, K. O. *Inorg. Chem.* **1979**, *18*, 2296.
(23) Davis, A. R.; Einstein, F. W. B. *Inorg. Chem.* **1980**, *19*, 1203.
(24) Pauling, L. *The Nature of the Chemical Bond*, 3rd ed.; Cornell: Ithaca, NY, 1960; p 257.

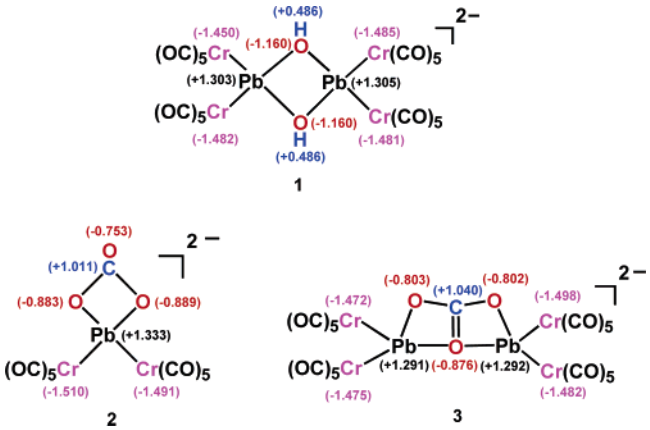

Figure 4. Natural charges for complexes **1**−**3**.

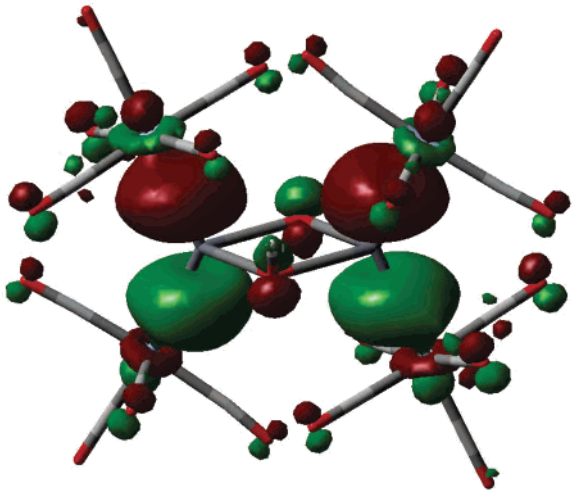

Figure 5. Isosurface of the highest-occupied molecular orbital of complex **1**.

DFT Calculations. The theoretical method of the density functional theory was employed in an attempt to better understand the nature of complexes **1**−**3** and the CO_2 absorption processes related to complex **1**. These calculations were carried out using the B3LYP DFT method with the LanL2DZ basis sets. The charges evaluated by the NBO method for complexes **1**−**3** are displayed in Figure 4. The analysis reveals that the charges on the Pb atoms in complexes **1**−**3** are +1.303/+1.305, +1.333, +1.291/+1.292, respectively. Similarly, the chromium atoms in **1**−**3** are found to carry charges of −1.4 to −1.5. Such modest ionic contributions support the interpretation of a significant covalent bonding character between the Pb atom and its coordinated $Cr(CO)_5$ groups, indicative of the strong bond between Pb and Cr found in complexes **1**−**3**, which is consistent with the X-ray data. In addition, the positively charged Pb atom also has great significance for the insertion of CO_2 into complex **1**. As shown in Figure 5, the HOMO of complex **1** was found to have a major contribution from the p orbitals of the Pb atoms, in addition to a certain contribution from the p orbitals of the O atoms in the OH^- groups. As a result, the electrophilic attack of the carbon of the inserting CO_2 is likely to occur at the O atom in the OH^- group accompanied by the O−Pb bond formation between the oxygen end of CO_2 and one of the two Pb atoms,

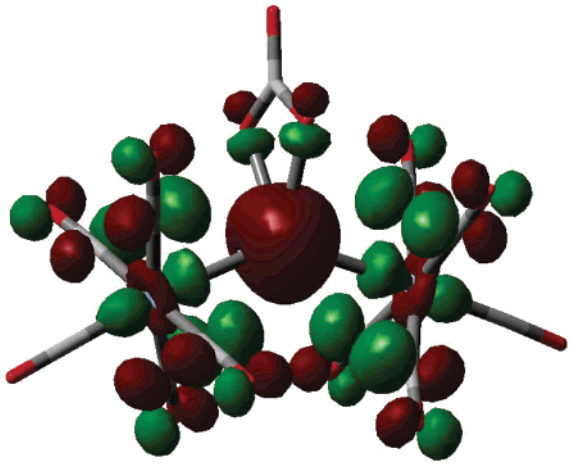

Figure 6. Isosurface of the lowest-unoccupied molecular orbital of complex **2**.

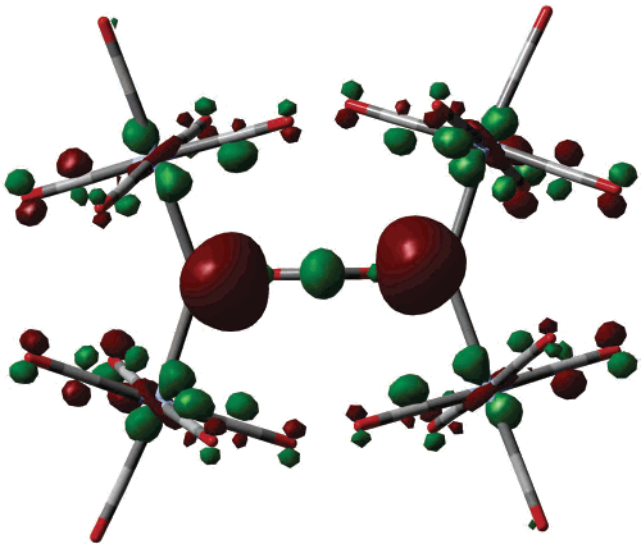

Figure 7. Isosurface of the lowest-unoccupied molecular orbital of complex **3**.

and hence, complex **2** is produced after the rest of the complex is detached. It is also interesting to note that the HOMO of the resulting complex (**2**) is mainly distributed over the Pb−CO_3^{2-} group (not shown) and the LUMO of complex **2** has a major contribution from the s orbital of the Pb atom (Figure 6). Therefore, complex **3** could be rationalized as a result of the intermolecular reaction by the nucleophilic attack of CO_3^{2-} from one of **2** on the Pb center of another **2**. On the other hand, the release of CO_3^{2-} from compounds **2** and **3** by the nucleophilic attack of the OH^- group could be related to the distribution of the LUMO of these two compounds. The LUMO of complexes **2** and **3** (Figures 6 and 7) each of which has a significant contribution from the s orbital of the Pb atom, suggests that OH^- is likely to nucleophilically attack at the Pb atom of complex **2** or **3** and form complex **1**, after the release of CO_3^{2-} by breaking the Pb−O bonds. Moreover, our experimental results show that upon the addition of OH^-, the conversion of **3** to **1** is more facile than **2** to **1**, which is also supported by simple energetic considerations via the theoretical calculations. The computational studies were done with the X-ray determined geometries of **1**−**3** and the OH^- and CO_3^{2-} geometries

optimized by the B3LYP/LanL2DZ method. Without consideration of the solvation effect and vibrational and rotational contributions, the reaction of complex **3** with OH^- to form complex **1** and CO_3^{2-} is favorable by 5.77 kcal/mol, while the reaction of complex **2** with OH^- is unfavorable by 113.33 kcal/mol. This result is consistent with the relatively facile transformation of **3** to **1** that was observed experimentally upon the addition of OH^-. On the basis of the experimental and theoretical results discussed above, the possibility that the reaction of **2** to **1** at the elevated temperature of 35 °C occurs by first converting **2** into **3** cannot be ruled out.

Conclusion

An unprecedented di-μ-hydroxo-lead−chromium carbonyl compound $[Et_4N]_2[\{PbCr_2(CO)_{10}\}_2(\mu\text{-}OH)_2]$ was synthesized and structurally characterized. The compound displays a high nucleophilicity toward gaseous CO_2 leading to the formation of novel κ^2OO- and μ-1κ^2OO′:2κ^2OO′-carbonato lead−chromium carbonyl complexes. The carbonato complexes can be reconverted back to the hydroxo complex under mild conditions. Molecular orbital calculations at the B3LYP level of the density function theory indicate that the Pb−O bonds of complex **1** are active sites for CO_2 fixation and the Pb centers of complexes **2** and **3** play the important role in the release of CO_3^{2-} upon the attack of the OH^- group.

Acknowledgment. This work was supported by the National Science Council of Taiwan (NSC Grant 93-2113-M-003-006 to M.S.). We are also grateful to the National Center for High-Performance Computing, where the Gaussian package and computer time were provided. Our gratitude also goes to the Academic Paper Editing Clinic, NTNU.

Supporting Information Available: X-ray crystallographic files in CIF format for $[TEBA]_2$[**1**], $[TMBA]_2$[**2**], and $[Et_4N]_2$[**3**], computational details for complexes **1**−**3**, and the optimized geometries of OH^- and CO_3^{2-}. This material is available free of charge via the Internet at http://pubs.acs.org.

IC060554O